Proceedings of the Thirtieth (2020) International Ocean and Polar Engineering Conference **www.isope.org**
Shanghai, China, October 11-16, 2020

ISBN 978-1-880653-84-5; ISSN 1098-6189

Three-dimensional Target Tracking Control for a Biomimetic Underwater Vehicle

Ge Bai, *Rui Wang*, *Yu Wang*, *Shuo Wang*
State Key Laboratory of Management and Control for Complex Systems,
Institute of Automation, Chinese Academy of Sciences
University of Chinese Academy of Sciences
Beijing, China

ABSTRACT

This paper presents a target tracking control method for a biomimetic underwater vehicle named RobCutt-II. The RobCutt-II is propelled by double undulatory fins which are distributed on both sides. In order to implement target tracking and observation in a certain distance, we propose a method by decoupling the target tracking control problem into distance, heading and depth control problems. Based on this idea, we design a target tracking controller composed of a navigation system, a distance controller, a heading controller, a depth controller and a switching logic controller. The simulation results verify the effectiveness of the proposed method on the biomimetic underwater vehicle.

KEY WORDS: Biomimetic underwater vehicle; active disturbance rejection control; target tracking; distance controller.

INTRODUCTION

Underwater vehicles play an important role in marine geological surveys and underwater rescue. Unlike traditional underwater vehicles driven by axial propellers, biomimetic underwater vehicles (BUVs) are propelled by undulatory fins for high mobility in complex underwater environments. Moreover, high stability, low noise, and small environmental disturbance are the advantages of biomimetic underwater vehicles compared with traditional underwater vehicles.

A variety of biomimetic underwater vehicles have been developed by scientists around the world. A BUV was designed by Delft University of Technology in the Netherlands (Simons, Bergers, Henrion, Hulzenga, Jutte, Pas, Van Schravendijk, Vercruyssen and Wilken, 2009). An undulatory fin propelled underwater vehicle was designed by Osaka University (Rahman, 2012). Zhou et al. from Nanyang Technological University developed a CPG-controlled underwater vehicle mimicking devil fish (Zhou and Low, 2012). In our previous work, we designed a biomimetic underwater vehicle propelled by undulatory fins named RobCutt-II (Wang, Wang and Wang, 2016). By means of different undulatory modes of the double fins, the RobCutt-II generates forces in the forward direction, vertical direction and moment to change the heading angle. However, the RobCutt-II cannot generate effective lateral force, which is considered as an underactuated system.

Many interesting method and results have been presented for underactuated systems. For example, Aguiar et al. proposed a control method for an underwater vehicle without lateral and vertical control (Aguiar and Pascoal, 2007). Yang et al. designed a robust trajectory tracking controller for marine surface vessels (Yang, Du, Liu, Guo and Abraham, 2014). Zhou et al. designed a path following method using the extended state observer and the neural network. (Peng, Wang and Han, 2019). In some underwater observation tasks, the underactuated underwater vehicles are required to track and to keep a certain distance from the target for observing. Existing researches pay little attention to this issue.

In this paper, a target tracking controller is designed to deal with the above problems. The controller, based on the Active Disturbances Rejection Control (ADRC), decouples the target tracking control problem into distance, heading and depth control problems. In order to reduce the coupling among distance, heading and depth control, the control output is selected by a switching logic controller. Simulations are performed in three different scenarios: stationary target tracking and observation, stationary target tracking under cross-flow disturbance, and moving target tracking under cross-flow disturbance. Finally, the three-dimensional target tracking tracking of the RobCutt-II is realized.

In the remainder of this paper, the biomimetic underwater vehicle platform and its mathematical model are introduced in Section II. The design of the target tracking controller is proposed in Section III and the target tracking controller is used for simulations in Section IV. Finally, the conclusion is presented in Section V.

OVERVIEW OF BUV ROBCUTT-II

As shown in Fig. 1, the biomimetic underwater vehicle named RobCutt-II is propelled by two biomimetic underwater propulsors on both sides (Wang, Wang, Wang, Tan and Yu, 2019). Each propulsor consists of a cylindrical cavity and an undulating long fin. With the coordinated control of the propagating waves, RobCutt-II can perform

many motions, including forward/backward motion, diving/floating motion, and rotation motion. The propagating waves are similar to sine waves and the frequency, amplitude, deflection angle, and phase difference of the waves are the control amount.

A camera is installed on the head of the RobCutt-II. It can be used to observe the target in front of the RobCutt-II, and to determine the distance d and the desired heading angle ψ_d between the RobCutt-II and the target. The heading angle ψ is measured by the inertial navigation fixed inside the RobCutt-II, and the depth z is measured by the pressure sensor installed below the underwater vehicle.

Fig. 1 Biomimetic underwater vehicle (RobCutt-II)

The kinematics model of the Robcutt-II in our previous work (Wang, Wang, Wang, Tang and Tan, 2018) can be expressed as

$$\begin{cases} \dot{x} = u\cos(\psi) - v\sin(\psi) \\ \dot{y} = u\sin(\psi) + v\cos(\psi) \\ \dot{z} = \omega \\ \dot{\psi} = r \\ M\dot{v} = -Cv - Dv + \tau + \tau_d \end{cases} \tag{1}$$

where $v=[u, v, \omega, r]^T$ is the velocity of the underwater vehicle in the body coordinate system $O_BX_BY_BZ_B$. The vector $[x, y, z, \psi]^T$ represents the position of the underwater vehicle in the world coordinate system $O_EX_EY_EZ_E$. $\tau=[\tau_u, 0, \tau_w, \tau_r]^T$ describes the vehicle-fixed propulsion force and moment, and $\tau_d=[\tau_{du}, \tau_{dv}, \tau_{dw}, \tau_{dr}]^T$ represents disturbance forces or moment acting on surge, sway and yaw. M, D and C are the rigid body system inertia matrix, the hydrodynamic damping matrix, and the Coriolis and centrifugal matrix respectively.

$$M = \begin{bmatrix} m_{11} & 0 & 0 & 0 \\ 0 & m_{22} & 0 & m_{24} \\ 0 & 0 & m_{33} & 0 \\ 0 & m_{42} & 0 & m_{44} \end{bmatrix}$$

$$D = \begin{bmatrix} d_{11} & 0 & 0 & 0 \\ 0 & d_{22} & 0 & d_{24} \\ 0 & 0 & d_{33} & 0 \\ 0 & d_{42} & 0 & d_{44} \end{bmatrix} \tag{2}$$

$$C = \begin{bmatrix} 0 & 0 & 0 & -m_{22}v - m_{24}r \\ 0 & 0 & 0 & m_{11}u \\ 0 & 0 & 0 & 0 \\ m_{22}v + m_{24}r & -m_{11}u & 0 & 0 \end{bmatrix}$$

where the parameters m_{xx} consist of mass and additional mass and the parameters d_{xx} are hydrodynamic damping coefficient. The readers can refer to (K. D. Do and J. Pan, 2009) for more details about the definitions of m_{11}, m_{22}, m_{33}, m_{44}, m_{24}, m_{42}, d_{11}, d_{22}, d_{33}, d_{44}, d_{24}, d_{42}.

TARGET TRACKING CONTROLLER

Framework of Target Tracking Controller

In order to control the RobCutt-II to track the underwater target and maintain a desired distance for observation, a target tracking controller is designed, which includes five modules: a navigation system, a distance controller, a heading controller, a depth controller and a switching logic controller. The framework of the target tracking controller is shown in Fig. 2. The Eq. 1 mentioned before is applied to the experimental model part - 'Biomimetic underwater vehicle'.

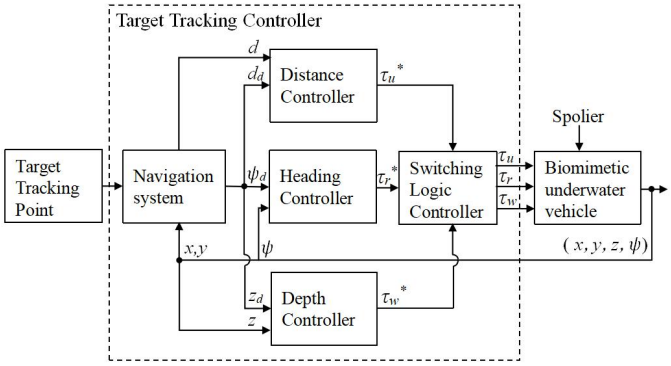

Fig. 2 Framework of the target tracking controller

Navigation system

The navigation system decouples the target tracking control problem into distance control, heading control, and depth control problems. The target trajectory point T $(x_{d(t)}, y_{d(t)}, z_{d(t)})$ (hereinafter written as (x_d, y_d, z_d), indicating the position of the target trajectory point on the present moment) is combined with the underwater vehicle's current position (x, y, z, ψ) to calculate the actual distance d and the desired heading angle ψ_d. Moreover, the desired distance d_d is given in different situations. The definitions of the related parameters are shown in Fig. 3.

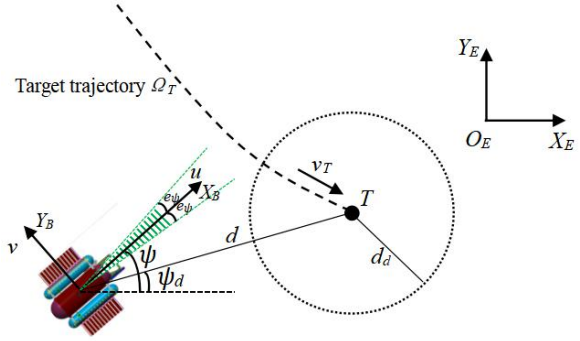

Fig. 3 Vertical view of target tracking

Distance controller

The distance controller is to make the Robcutt-II reach and maintain a desired distance from the target trajectory point. The input of the distance controller is the desired distance d_d and the actual distance d. It should be noted that d_d and d are the distance in the vertical view. The desired distance d_d >0 is artificially given. The actual distance d is the horizontal distance between the current position (x, y, z) and the desired target trajectory point T (x_d, y_d, z_d), which is defined as follows:

$$d = \sqrt{(x - x_d)^2 + (y - y_d)^2} \tag{3}$$

Based on the definition of d, the derivative of d is

$$\dot{d} = \frac{(x - x_d)\dot{x} + (y - y_d)\dot{y}}{\sqrt{(x - x_d)^2 + (y - y_d)^2}} \tag{4}$$

The kinematics model of the RobCutt-II is given in Eq. 1, so the derivatives of x and y are

$$\begin{aligned} \dot{x} &= u\cos(\psi) - v\sin(\psi) \\ \dot{y} &= u\sin(\psi) + v\cos(\psi) \end{aligned} \tag{5}$$

In Fig. 3, the formula of the desired heading angle ψ_d is

$$\begin{aligned} \cos(\psi_d) &= \frac{-(x - x_d)}{\sqrt{(x - x_d)^2 + (y - y_d)^2}} \\ \sin(\psi_d) &= \frac{-(y - y_d)}{\sqrt{(x - x_d)^2 + (y - y_d)^2}} \end{aligned} \tag{6}$$

The derivative of d is reduced to

$$\begin{aligned} \dot{d} &= -(u\cos(\psi) - v\sin(\psi))\cos(\psi_d) - (u\sin(\psi) + v\cos(\psi))\sin(\psi_d) \\ &= -u\cos(\psi - \psi_d) + v\sin(\psi - \psi_d) \end{aligned} \tag{7}$$

It is obvious that $\dot{d} \approx -u$ when $|\psi - \psi_d| \approx 0$. Therefore, the kinematics model of the distance control channel is finally described as:

$$\begin{cases} \dot{d} \approx -u \\ \dot{u} = \dfrac{m_{22}}{m_{11}} vr + \dfrac{m_{24}}{m_{11}} r^2 - \dfrac{d_{11}}{m_{11}} u + \dfrac{1}{m_{11}} \tau_{du} + \dfrac{1}{m_{11}} \tau_u^* \end{cases} \tag{8}$$

The formula can be rewritten as ($|\psi - \psi_d| \approx 0$):

$$\dot{d} = f_u + \frac{d_{11}}{m_{11}} u - \frac{1}{m_{11}} \tau_u^* \tag{9}$$

where $f_u = -\left(\dfrac{m_{22}}{m_{11}} vr + \dfrac{m_{24}}{m_{11}} r^2 + \dfrac{1}{m_{11}} \tau_{du} \right)$ represents the coriolis, centripetal and unknown disturbing forces of the distance channel.

As shown in Fig. 4, the tracking differentiator (TD) is used to obtain the tracking signal d_1 and definition signal d_2 from a desired distance d_d. The state variables ζ_{d1}, ζ_{d2} and ζ_{d3} of the extended state observer (ESO) separately estimates d, $\dot{d}$ (i.e. -u) and f_u .

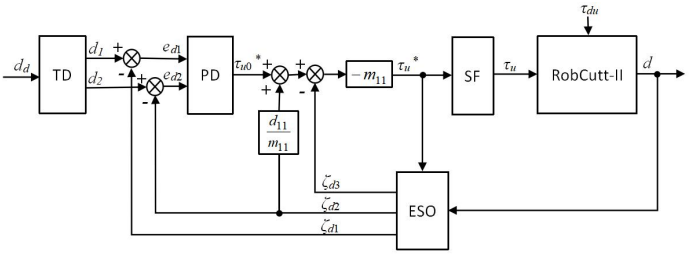

Fig. 4 Block diagram of ADRC controller

The control algorithm is designed as:

$$\tau_u^* = (-m_{11}) \left(-\zeta_{d3} + \frac{d_{11}}{m_{11}} \zeta_{d2} + \tau_{u0}^* \right) \tag{10}$$

The system can be reduced to a second-order integrator system

$$\ddot{d} = (f_u - \zeta_{d3}) + \frac{d_{11}}{m_{11}} (u + \zeta_{d2}) + \tau_{u0}^* \approx \tau_{u0}^* \tag{11}$$

A proportion differentiation (PD) controller can be used to control the Robcutt-II

$$\tau_{u0}^* = k_{up} e_{u1} + k_{ud} e_{u2} \tag{12}$$

Therefore, The linear discrete ADRC distance controller can be summarized as follows. The definition of the 'fhan' function can be found in the ref. (Han, 2007).

$$\begin{cases} d_1(k+1) = d_1(k) + h_d d_2(k) \\ d_2(k+1) = d_2(k) + h_d \cdot \mathrm{fhan}(d_1(k) - d_d(k), d_2(k), r_d, h_{d0}) \\ e_d = \zeta_{d1}(k) - d(k) \\ \zeta_{d1}(k+1) = \zeta_{d1}(k) + h_d (\zeta_{d2}(k) - 3\omega_{od} e_d) \\ \zeta_{d2}(k+1) = \zeta_{d2}(k) + h_d (\zeta_{d3}(k) - \dfrac{d_{11}}{m_{11}} \zeta_{d2}(k) - \dfrac{1}{m_{11}} \tau_u^* - 3\omega_{od}^2 e_d) \\ \zeta_{d3}(k+1) = \zeta_{d3}(k) - h_d \omega_{od}^3 e_d \\ e_{u1} = d_1(k+1) - \zeta_{d1}(k+1) \\ e_{u2} = d_2(k+1) - \zeta_{d2}(k+1) \\ \tau_{u0}^* = k_{up} e_{u1} + k_{ud} e_{u2} \\ \tau_u^* = (-m_{11}) \left(-\zeta_{d3} + \dfrac{d_{11}}{m_{11}} \zeta_{d2} + \tau_{u0}^* \right) \end{cases} \tag{13}$$

Heading Controller and Depth Controller

The input of the heading controller is the desired heading angle ψ_d and the actual heading angle ψ. The actual heading angle ψ is defined as the angle between the O_BX_B axis and the O_EX_E axis, which is in the range of [0, 2π). A ray is formed by the current position (x, y, z) and the desired target trajectory point T (x_d, y_d, z_d). The desired heading angle ψ_d is defined as the angle between the ray and the O_EX_E axis, which can be specifically expressed as:

$$\psi_d = \begin{cases} \arccos\left(\dfrac{(x_d - x, y_d - y)\cdot(1,0)}{\sqrt{(x_d - x)^2 + (y_d - y)^2}\sqrt{1^2 + 0^2}}\right) & (y_d - y) \geq 0 \\ 2\pi - \arccos\left(\dfrac{(x_d - x, y_d - y)\cdot(1,0)}{\sqrt{(x_d - x)^2 + (y_d - y)^2}\sqrt{1^2 + 0^2}}\right) & (y_d - y) < 0 \end{cases} \tag{14}$$

When the positive direction of the $O_E X_E$ axis is surrounded by the desired heading angle ψ_d and the actual heading angle ψ, ψ and ψ_d cannot be simply used as the input of the heading controller, because the appropriate range of $|\psi_d - \psi|$ is $[0, \pi)$. Therefore, the following algorithm is designed to correct the desired heading angle ψ_d:

Algorithm 1: The algorithm of the desired heading angle ψ_d correction

1: Calculate and compare $|\psi - \psi_d|$, $|\psi - (\psi_d - 2\pi)|$, $|\psi - (\psi_d + 2\pi)|$;
2: **if** ($|\psi - (\psi_d - 2\pi)|$ is the minimum) **then**
3: $\psi_d = (\psi_d - 2\pi)$;
4: **else if** ($|\psi - (\psi_d + 2\pi)|$ is the minimum) **then**
5: $\psi_d = (\psi_d + 2\pi)$;
6: **else**
7: ψ_d is unchanged;
8: **end if**

Combined with the kinematics model, the algorithm of heading control is as follows:

$$\begin{cases} \dot{\psi} = r \\ \dot{r} = -\dfrac{m_{42}}{m_{44}}\dot{v} - \dfrac{d_{42}}{m_{44}}v - \dfrac{d_{44}}{m_{44}}r - \dfrac{m_{24}}{m_{44}}vr \\ \qquad + \dfrac{d_{42} - m_{22}}{m_{44}}uv + \dfrac{1}{m_{44}}\tau_{dr} + \dfrac{1}{m_{44}}\tau_r \end{cases} \tag{15}$$

The heading controller is designed based on the Active Disturbances Rejection Control (ADRC). In the heading controller, the desired heading angle ψ_d is used as the tracking amount of the tracking differentiator, the actual heading angle ψ is used as the observation of the extended state observer and the error feedback is applied to obtain the virtual control moment τ_r. The specific method of the heading controller can be found in the literature (Wang, Wang and Wang, 2016).

As in the above case, the algorithm of depth control is as follows:

$$\begin{cases} \dot{z} = w \\ \dot{w} = -\dfrac{d_{33}}{m_{33}}w + \dfrac{1}{m_{33}}\tau_{dw} + \dfrac{1}{m_{33}}\tau_w \end{cases} \tag{16}$$

The depth controller is also designed based on ADRC. The inputs are desired depth z_d, actual depth z. The desired depth z_d is the z_d of the target trajectory point $T(x_d, y_d, z_d)$, and the actual depth z is the z of the current position (x, y, z). As same as the heading controller, z_d and z are the tracking amount of the tracking differentiator and the observation of the extended state observer and the virtual heave control force τ_w is obtained. The design method of the depth controller is in the literature (Wang, Wang, Wang, Tan and Yu, 2019).

Switching Logic Controller

In order to track the target trajectory point and to reach the desired distance d_d, the algorithm for designing the propulsive control force τ_u is as follows:

$$\tau_u = \tau_u^* \cdot \lambda_{\tau r} \cdot \lambda_z \tag{17}$$

Assuming that the depth z direction has reached desired value and the critical value of heading angle deviation e_ψ is a small positive value, the following strategy is designed in connection with Fig. 3 and Eq. 6:

If $|\psi - \psi_d| > e_\psi$, the forward control amount $\tau_r = 0$ and the heading control amount τ_r is the only output.

If $|\psi - \psi_d| \leq e_\psi$, $|\psi - \psi_d| \approx 0$, $\dot{d} \approx -u$ the propulsive control amount τ_u can be used as the control amount. At this time, both τ_r and τ_u are output. In this case, the desired distance d_d ($d_d > 0$) is known. By changing the propulsive control amount τ_u continuously, the actual distance d can gradually approach the desired distance d_d, and the goal of tracking the target point is achieved.

Based on this idea, the heading angle adjustment parameter $\lambda_{\tau r}$ is defined. The value of the $\lambda_{\tau r}$ is 0 or 1. As shown in Fig. 5, the critical value of heading angle deviation e_ψ is composed of $e_{\psi L}$ and $e_{\psi U}$, which represents the critical value of heading angle deviation toward (blue line) and away from the target (red line). This method can avoid changing τ_u repeatedly when $|\psi - \psi_d| \approx e_\psi$.

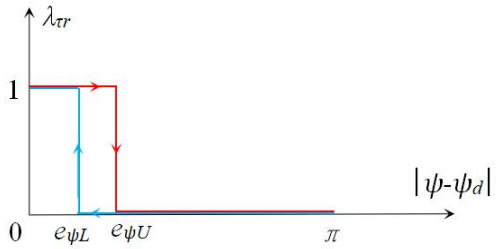

Fig. 5 Variation of heading angle adjustment parameter $\lambda_{\tau r}$ with $|\psi - \psi_d|$.

During the actual movement of the underwater vehicle, there is a strong coupling between the propulsive force τ_u and the heave force τ_w. In order to reduce the effect of the coupling, τ_u decreases with the increase of the depth deviation. Therefore, the depth adjustment parameter λ_z is defined as follows:

$$\lambda_z = \frac{1}{k_z e_z + 1} \tag{18}$$

Among them, the depth deviation $e_z = |z - z_d|$. k_z ($k_z > 0$) is a depth and forward coupling adjustment coefficient, which is used to characterize the amplitude of the depth deviation on the propulsive force. Based on the above ideas, a switching logic controller algorithm is designed as follows:

Algorithm 2: The algorithm of the switching logic controller

1: The virtual controllers τ_u^*, the critical value of heading angle deviation $e_{\psi L}$, $e_{\psi U}$ ($0 < e_{\psi L} < e_{\psi U}$), the depth and forward coupling adjustment coefficient k_z ($k_z > 0$) are given;
2: **if** (the heading direction is toward the target point) **then**
3: $e_\psi = e_{\psi L}$;
4: **else**
5: $e_\psi = e_{\psi U}$;
6: **end if**
7: **if** ($|\psi - \psi_d| > e_\psi$) **then**
8: $\lambda_{\tau r} = 0$;

9: **else**
10: $\lambda_{\tau r}$=1;
11: **end if**
12: $\lambda_z = \frac{1}{k_z e_z + 1} = \frac{1}{k_z |z - z_d| + 1}$;
13: $\tau_u = \tau_u^* \cdot \lambda_{\tau r} \cdot \lambda_z$;

When the deviation of distance, heading, or depth is too large, the value of the control amount τ_u, τ_r or τ_w is unable to control. For this reason, the propulsive, heading, and heave critical control value τ_{umax}, τ_{rmax}, τ_{wmax} are added to get the actual control amount τ_u, τ_r and τ_w .

UNDERWATER TARGET TRACKING SIMULATION ANALYSIS

With the target tracking controller introduced in Chapter 3, three different simulation experiments are designed, including stationary target tracking and observation, stationary target tracking under cross-flow disturbance, and moving target tracking under cross-flow disturbance. The control variables in the simulation are τ_u, τ_w, τ_r. The actual control amount of the underwater vehicle are the amplitude, frequency, offset angle and phase difference of the waveform. The relationship can be obtained by the traveling wave parameter mapping model based on fuzzy inference in the literature (Wang, Wang and Wang, 2016).

Stationary target tracking

Aiming at the stationary target tracking and observation, in order to verify the effectiveness of the target tracking controller proposed in this paper, the model is simulated and analyzed with MATLAB. The model parameters are selected as m_{11} = 57.5, m_{22} = 61.3, m_{33} = 61.3, m_{44} = 1.15, d_{11} = 53, d_{22} = 58, d_{33} = 70, d_{44} = 3.1, $m_{24} = m_{42} = d_{24} = d_{42} = 0$. In the navigation system, the desired distance d_d is 0.2m, the control period δ_z is 0.02s, and the simulation time is 50s.

It is assumed that the underwater vehicle is affected by the external interference in three different directions. The interference model are $\tau_{du}(t) = 3 \cdot randn$, $\tau_{dw}(t) = 3 \cdot randn$ and $\tau_{dr}(t) = 0.5 \cdot randn$, where *randn* represents standard normal distribution numbers. In the distance controller, the control parameters are as follows: the speed factor r = 0.2, the filter factor h_{z0} = 0.04, the extended state observer parameter ω_c = 3 and the error feedback parameters k_p = 900, k_d = 72. The initial position is (1, -1, 0) and the position of the stationary target point is (0,0, -0.5). The simulation result is shown in Fig. 6.

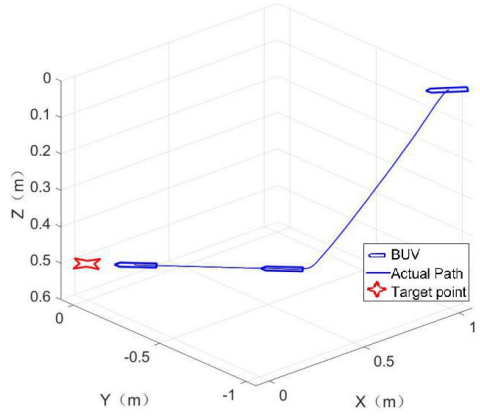

Fig. 6 Stationary target tracking

It can be known that the underwater vehicle can track and maintain a certain distance from the stationary target in the case of disturbance. Fig. 7 is the time evolution of the distance, angle difference and depth of the underwater vehicle to the target point. Although the vehicle is affected by external disturbances during the movement, the distance, the angle difference and the depth from the target point are basically not affected with the target tracking controller, which indicates that the target tracking controller in this article has strong anti-interference ability. Fig. 8 shows the control quantities τ_u, τ_w, τ_r of the underwater vehicle.

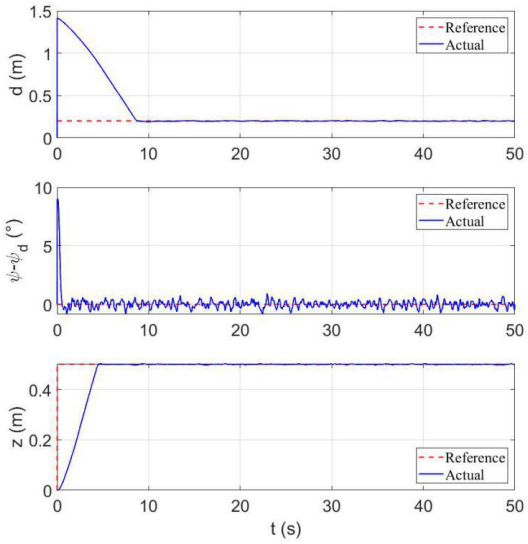

Fig. 7 Time evolution of the reference and actual position parameter in the stationary target tracking

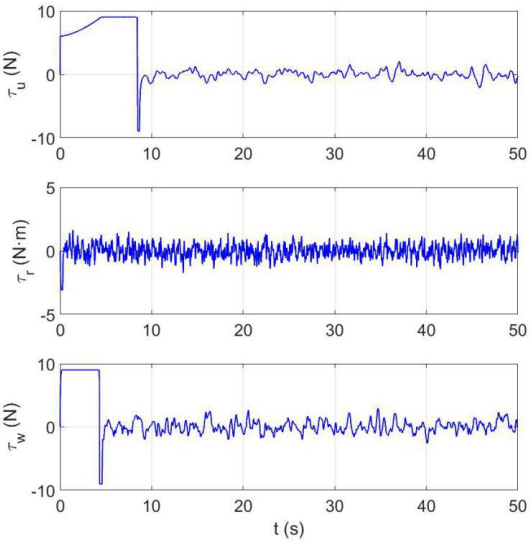

Fig. 8 Time evolution of the control amount in the stationary target tracking

In addition, a stationary target tracking simulation is carried out under the cross-flow disturbances. As the model above, a cross-flow disturbance is added with an angle of 90° counterclockwise to the X_E axis and the velocity is 0.02 m/s. The result is shown in Fig. 9.

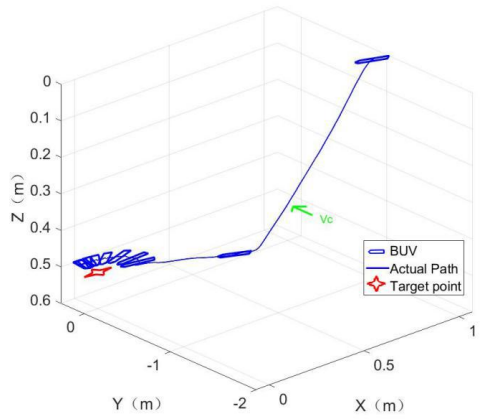

Fig. 9 Stationary target tracking under cross-flow disturbance

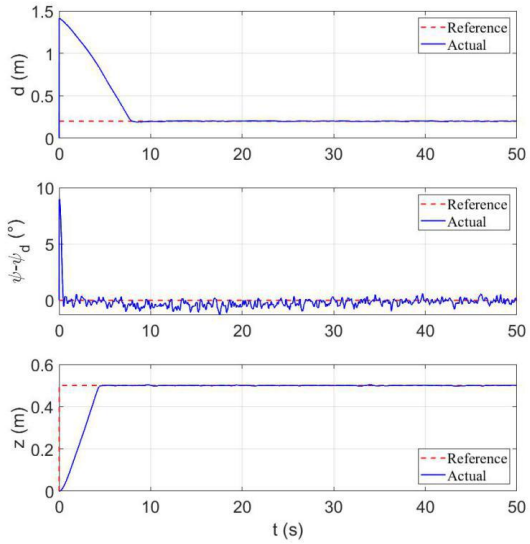

Fig. 10 Time evolution of the reference and actual position parameter in the stationary target tracking under cross-flow disturbance

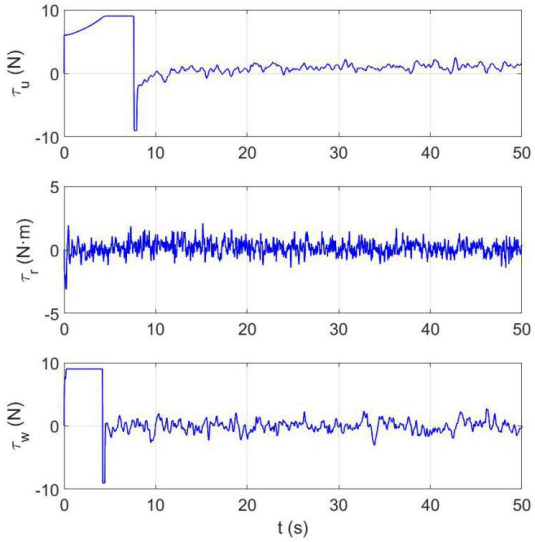

Fig. 11 Time evolution of the control amount in the stationary target tracking under cross-flow disturbance

In the case of cross-flow disturbances, the underwater vehicle can track and maintain a certain distance from the stationary target, but cannot maintain a certain angle in the heading direction. Because the Robcutt-II is an underactuated underwater system, the control force in the Y_B direction of the body-fixed coordinate system is 0, which means that there is no anti-interference in the Y_B direction. Therefore, the vehicle ultimately maintains the direction opposite to the cross-flow direction. The simulation results are shown in Fig. 10 and 11.

Moving target tracking

For the moving target, the trajectory is designed as an S-shaped curve, the initial position is (0.92, -2.2, 0.5) and the final position is (2.24, -0.5, 0.3). The target point moves at a uniform speed of 0.12 m/s and the simulation time is 500s.

The conditions are the same as described above, assuming that the Robcutt-II is affected by external interference in three directions and the interference model are $\tau_{du}(t) = 3 \cdot randn$, $\tau_{dw}(t) = 3 \cdot randn$ and $\tau_{dr}(t) = 0.5 \cdot randn$. At the same time, a cross-flow disturbance is added with an angle of 90° counterclockwise to the X_E axis and the velocity is 0.02 m/s. The simulation result is shown in Fig. 12.

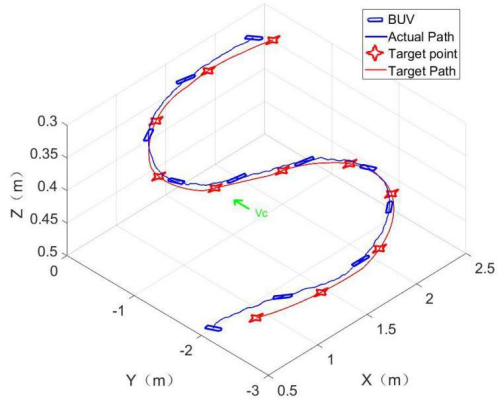

Fig. 12 Moving target tracking under cross-flow disturbance

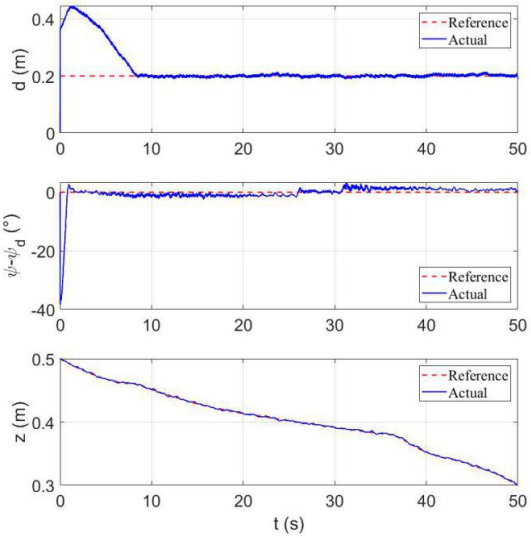

Fig. 13 Time evolution of the reference and actual position parameter in the moving target tracking under cross-flow disturbance

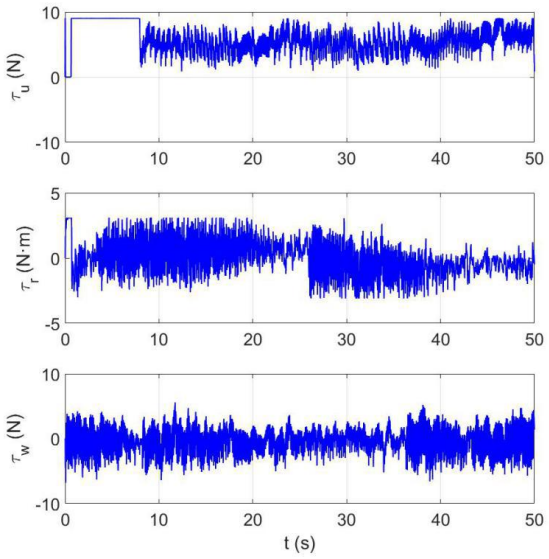

Fig. 14 Time evolution of the control amount in the stationary target tracking under cross-flow disturbance

Under the circumstances of the external interference and the cross-flow disturbance, the Robcutt-II can also track the moving target well. Fig. 13 shows the time evolution of the reference and actual position parameter in the moving target tracking under cross-flow disturbance and Fig.14 shows the time evolution of the control amount in the stationary target tracking under cross-flow disturbance. In order to track the target point as sensitively as possible, The control amount $\tau=[\tau_u, 0, \tau_w, \tau_r]^T$ changes drastically in Fig.14 which is affected by the interference $\tau_d=[\tau_{du}, \tau_{dv}, \tau_{dw}, \tau_{dr}]^T$. It can be seen that the tracking distance, depth, and yaw angle are consistent with the desired distance, desired depth, and desired heading angle, indicating that the target tracking controller is credible.

CONCLUSIONS

The target tracking controller of a BUV has been achieved. Specially, the target tracking problem was decoupled into three control problems. Furthermore, a distance controller, a heading controller and a depth controller were designed respectively. Then a switching logic controller was designed to coordinate the outputs of three sub-controllers. Simulations were performed for stationary target tracking and moving target tracking under cross-flow disturbance. The results verify the validity of the proposed target tracking controller.

ACKNOWLEDGEMENTS

This work was supported in part by the National Natural Science Foundation of China under Grant U1713222, and U1806204, and in part by the Equipment Pre-research Field Fund under Grant 61403120407. Corresponding author: Dr. Rui Wang (rwang5212@ia.ac.cn).

REFERENCES

Aguiar AP and Pascoal AM (2007). "Dynamic positioning and way-point tracking of underactuated AUVs in the presence of ocean currents," *International Journal of Control*, 80, 1092-1108.

Han, JQ (2007). "Auto Disturbances Rejection Control Technique ADRC," *Beijing: National Defense Industry Press*

K. D. Do and J. Pan, "Control of Ships and Underwater Vehicles," *London, England: Springer*, 2009.

Peng, ZH, Wang J and Han QL (2019). "Path-Following Control of Autonomous Underwater Vehicles Subject to Velocity and Input Constraints via Neurodynamic Optimization," *IEEE Transactions on Industrial Electronics*, Vol 66, 8724-8732.

Rahman M (2012). "Study on biomimetic squid-like underwater robots with two undulating side fins," *Osaka University Library*

Simons DG, Bergers MMC, Henrion S, Hulzenga JIJ, Jutte RW, Pas WMG, Van Schravendijk M, Vercruyssen TGA and Wilken AP (2009). "A highly versatile autonomous underwater vehicle with biomechanical propulsion," *Proceedings OCEANS' 09*, 1-6.

Wang R, Wang S and Wang Y (2016). "A Hybrid Heading Control Scheme for a Biomimetic Underwater Vehicle," *Proceedings of 26th Int. Ocean Polar Eng. Conference*, Greece, 619-625.

Wang R, Wang S, Wang Y, Tang C and Tan M (2018). "Three-Dimensional Helical Path Following of an Underwater Biomimetic Vehicle-Manipulator System," *IEEE Journal of Oceanic Engineering*, Vol 43, 391-401.

Wang R, Wang S, Wang Y, Tan M and Yu JZ (2019). "A Paradigm for Path Following Control of a Ribbon-Fin Propelled Biomimetic Underwater Vehicle," *IEEE Transactions on Systems, Man, and Cybernetics: Systems*, Vol 49, 482-493.

Yang Y, Du JL, Liu HB, Guo C, and Ajith Abraham (2014). "A Trajectory Tracking Robust Controller of Surface Vessels With Disturbance Uncertainties," *IEEE Transactions on Control Systems Technology*, Vol 22, 1511-1518.

Zhou CL and K. H. Low (2012). "Design and Locomotion Control of a Biomimetic Underwater Vehicle With Fin Propulsion," *IEEE/ASME Transactions on Mechatronics*, Vol 17, 25-35.